

Design of erythrocyte-derived carriers for bioimaging applications

Wing-Fu Lai,^{1,2,*} Dahong Zhang,² and Wing-Tak Wong¹

Abstract

Erythrocytes are physiological entities that have been exploited in both preclinical and clinical trials for the delivery of exogenous agents. Over the years, diverse erythrocyte-derived carriers (ECs) have been developed with related patents granted for industrial and commercial purposes. However, most ECs have only been exploited for drug delivery. Serious discussions regarding their applications in imaging are scarce. This article reviews the role of ECs in enhancing imaging efficiency and subsequently delineates strategies for engineering and optimising their preclinical and clinical performance. With a snapshot of the latest developments and use of ECs in imaging, directions to streamline the clinical translation of related technologies can be attained for future research.

Use of ECs in delivery research

ECs show several favourable features that cannot be surpassed by existing carriers. Compared with synthetic nanoparticles, including nanogels [15–19], metal nanoparticles [20,21], and lipid-based nanoparticles [22–25], which may be recognised by the body as foreign substances and eliminated easily by immune reactions, ECs can be generated from host-originated erythrocytes and have longer blood circulation time without eliciting immune responses. Compared with proteinaceous systems, such as ferritin [26] and hepatitis B virus core protein [27], which are potentially immunogenic and require tedious procedures for fabrication or purification, erythrocytes can be obtained from the host via blood withdrawal. Furthermore, ECs are easily accessible and can be generated on a large scale. Along with their intrinsic biocompatibility [28], ECs have attracted extensive interest in delivery research [29–32], and research on several ECs has progressed to clinical trials. To date, ECs are tested as carriers of copious therapeutic agents, including L-asparaginase [33], adenosine deaminase [34], dexamethasone 21-phosphate [35], and thymidine phosphorylase [36], to treat diverse diseases, ranging from severe combined immunodeficiency [34] and ataxia telangiectasia [35] to cancer [37].

In the past few decades, extensive efforts have been made to exploit ECs for the delivery of therapeutic agents; however, the use of ECs in diagnostic procedures such as imaging has not been studied. Similar to therapeutic agents, imaging agents can be loaded into ECs either by attachment to the carrier surface or encapsulation in the carrier (Box 1). Existing advances

in EC-mediated drug delivery can be readily translated into the development of EC-delivered imaging agents (EIAs). This review delineates the major roles played by ECs in bioimaging and subsequently discusses various strategies for enhancing and optimising carriers for preclinical and clinical applications. The objective of this review is to provide a snapshot of the latest advances in the development of ECs for application in imaging and to highlight the unmet needs for the translation of related technologies from the laboratory to the clinical context.

Box 1. Strategies for fabricating EIAs

One strategy for generating EIAs is to attach an imaging agent to the erythrocyte surface (Figure I). This method, however, can change the surface properties of ECs and may interfere with the functioning and survival of the erythrocytes. Another strategy is to have the imaging agent physically entrapped inside the ECs. One of the commonly used methods for this is hypotonic treatment, in which erythrocytes are placed in a hypotonic solution. When the osmotic pressure of the solution is lower than that of the erythrocyte, haemolysis occurs, forming pores on the erythrocyte membrane with diameters of 10–500 nm [90]. This approach has been adopted to generate erythrocyte membrane-coated gold nanoparticles. During the fabrication process, erythrocytes are obtained from whole blood via centrifugation and are subjected to hypotonic medium treatment [46]. The generated erythrocyte ghosts are then extruded after sonication through polycarbonate porous membranes to produce erythrocyte-derived vesicles [46], which can be used to coat citrate-stabilised gold nanoparticles to enable immune evasion [46]. An approach similar to the hypotonic medium treatment was applied to coat docetaxel-loaded IR780-containing polymeric nanoparticles with erythrocyte membranes to generate an imaging probe that can mediate fluorescence and PAI and simultaneously mediate phototherapy and chemotherapy of tumours [39].

Apart from the conventional hypotonic medium treatment, related working principles have been modified over the years, leading to the development of different methods, including hypotonic dialysis [91], hypotonic preswelling [92], and hypotonic dilution [93], for the generation of EIAs. Recently, a red cell loader, which comprises a continuous flow centrifuge, vacuum pump, and haemofilter for the concentration of lysed erythrocytes, was also developed for automated agent loading into erythrocytes [94]. Apart from relying on the hypotonic medium treatment, membrane disruption can be achieved via electroporation and chemical perturbation during the fabrication of EIAs [95,96]. Besides disrupting the plasma membrane of the erythrocyte, imaging agents can first be loaded into effector-containing lipid vesicles and subsequently fused with the erythrocyte for loading purposes. This method was adopted to incorporate inositol hexaphosphate into intact erythrocytes [97]. In addition, upon conjugation of an agent with receptor- and transporter-independent membrane-translocating peptides, the agent can get into the erythrocytes [98]. All these strategies can be applied to fabricate EIAs for different imaging modalities.

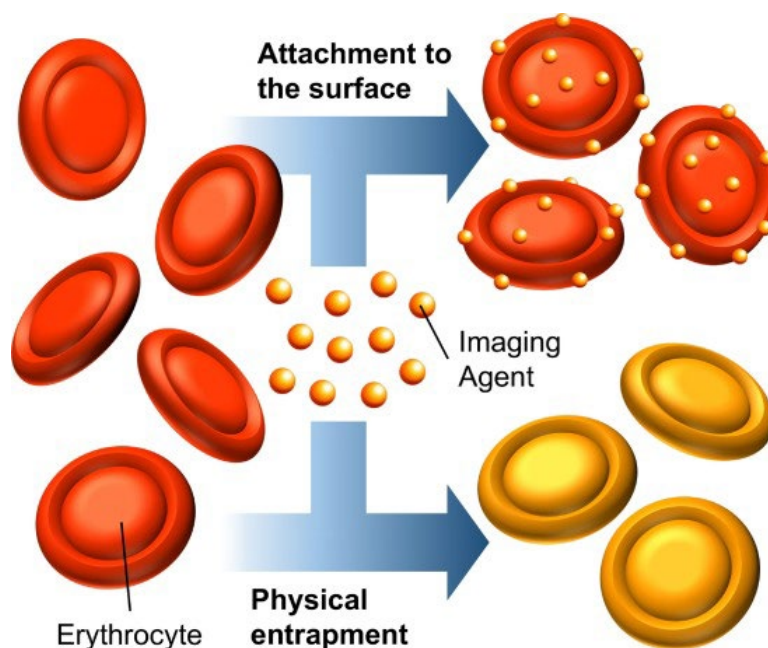


Figure I. Major methods of EIA fabrication.

Roles played by ECs in imaging

ECs often augment the efficiency of imaging procedures compared with that achieved using free imaging agents [38]. In general, ECs play two roles in the imaging process. First, they enhance the biocompatibility and stability of the imaging agent to make it last longer inside the body. Second, they manipulate the distribution of the imaging agent to enable more effective imaging of the target tissue.

Enhancing the biocompatibility and stability of an imaging agent

The ability of ECs to enhance the blood circulation time of an imaging agent was demonstrated in a recent study [39]. The study adopted high-pressure homogenisation to generate nanoparticles consisting of poly(caprolactone) (PCL) and polyethylene glycol (PEG) in a PCL–PEG–PCL (PCEC) tri-block copolymer coloaded with docetaxel and IR780 iodide. Subsequently, the nanoparticles were coated with erythrocyte membranes to obtain multifunctional nanoparticles for *in vivo* administration (Figure 1) [39]. Compared with their unmodified counterparts, coated nanoparticles have prolonged blood circulation [39]. In addition, during fluorescence imaging, the fluorescence intensity of tumours in mice treated with coated nanoparticles was higher than that for mice treated with unmodified nanoparticles [39]. Similarly, during photoacoustic imaging (PAI), the signals of tumours treated with nanoparticles were enhanced after coating the nanoparticles with erythrocyte membranes [39]. This may be because the coating enhanced the immune stealth ability of the imaging agent against macrophages [40]. Irrespective, for EIAs to undergo immune evasion, preserving the CD47 on the erythrocyte membrane is a prerequisite [38]. Therefore, carefully designing the coating protocol to confirm the erythrocyte membrane sidedness is crucial.

ECs can enhance the biocompatibility and stability of the imaging agent as demonstrated using a poly(lactic-co-glycolic acid) (PLGA) core labelled with a lipid-conjugated gadolinium-based molecular contrast agent [38]. Coating the core with an erythrocyte membrane enhanced its stability in serum by limiting the absorption of proteins onto the core surface [38], and minimised transmetalation of the core with endogenous scavenger cations (zinc, iron, and copper) in blood circulation [38]. A similar effect of erythrocyte membrane concealment was reported by Xiao *et al.* [40], who found that the agent exhibited a lower rate of haemolysis after being coated with an erythrocyte membrane [40]. This corroborates the effect of ECs for enhancing the safety profile of the imaging agent.

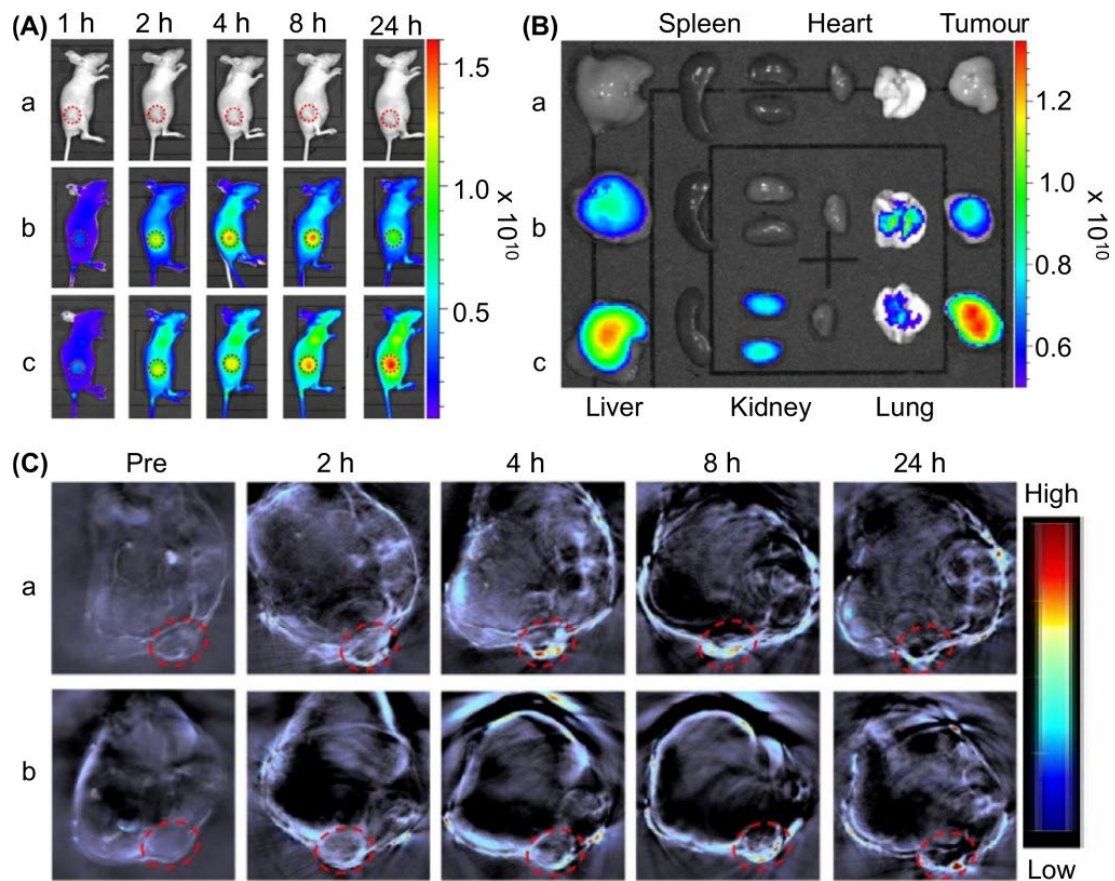


Figure 1. The *in vivo* performance of erythrocyte-camouflaged docetaxel/IR780 coloaded nanoparticles in tumour-bearing mice.

(A) Fluorescence imaging of the tumour-bearing mice treated with (a) saline solution, (b) unmodified docetaxel/IR780 coloaded nanoparticles, and (c) erythrocyte-camouflaged docetaxel/IR780 coloaded nanoparticles. The red circles indicate the tumour regions. (B) *Ex vivo* fluorescence imaging of tumours and organs harvested from mice 24 h post-injection of (a) saline solution, (b) unmodified docetaxel/IR780 coloaded nanoparticles, and (c) erythrocyte-camouflaged docetaxel/IR780 coloaded nanoparticles. (C) Photoacoustic imaging of tumour-bearing mice treated with (a) unmodified docetaxel/IR780 coloaded nanoparticles and (b) erythrocyte-camouflaged docetaxel/IR780 coloaded nanoparticles. Reproduced, with permission, from

[39].

Altering the biodistribution of an imaging agent

In addition to biocompatibility and stability, the biodistribution profile of an imaging agent can be altered by ECs. This was demonstrated in a recent study [41] in which splenectomised NOD scid gamma (NSG) immunodeficient mice were injected intravenously with either free 2-deoxy-2- ^{18}F fluoro-D-glucose (FDG) or FDG-labelled erythrocytes. Electrocardiography-gated micro-positron emission tomography (microPET)/computed tomography (CT) imaging revealed that free FDG largely accumulates in the myocardium and brain (Figure 2) [41]. Upon loading into erythrocytes, FDG signals were observed mainly in large vessels of the body and detected in major organs (e.g., heart, lungs, liver, spleen, and kidneys) [41]. Fused microPET/CT images of the heart showed myocardial uptake of free FDG in the left ventricle of mice injected with free FDG. By contrast, FDG activity in mice injected with FDG-

labelled erythrocytes was found predominantly con-fined to the intraluminal chambers of the heart [41]. This demonstrated the effect of erythrocytemembrane concealment on the spatial distribution of imaging signals. Based on this effect, re- cently, it was proposed that lipid–polymer paramagnetic nanoparticles should be coated with erythrocyte membranes for use in magnetic resonance imaging (MRI) [38]. The coated nano- particles were found to have a circulation half-life of approximately 12 h after intravenous admin-istration to mice [38] and accumulated largely in highly vascularised organs (e.g., liver and spleen) with little accumulation in the lungs, bones, and kidneys [38]. By contrast, Magnevist accumu- lated mainly in the kidneys [38] and was more prone to elimination than coated nanoparticles. This demonstrates the application potential of ECs in manipulating the biodistribution profiles of imaging probes.

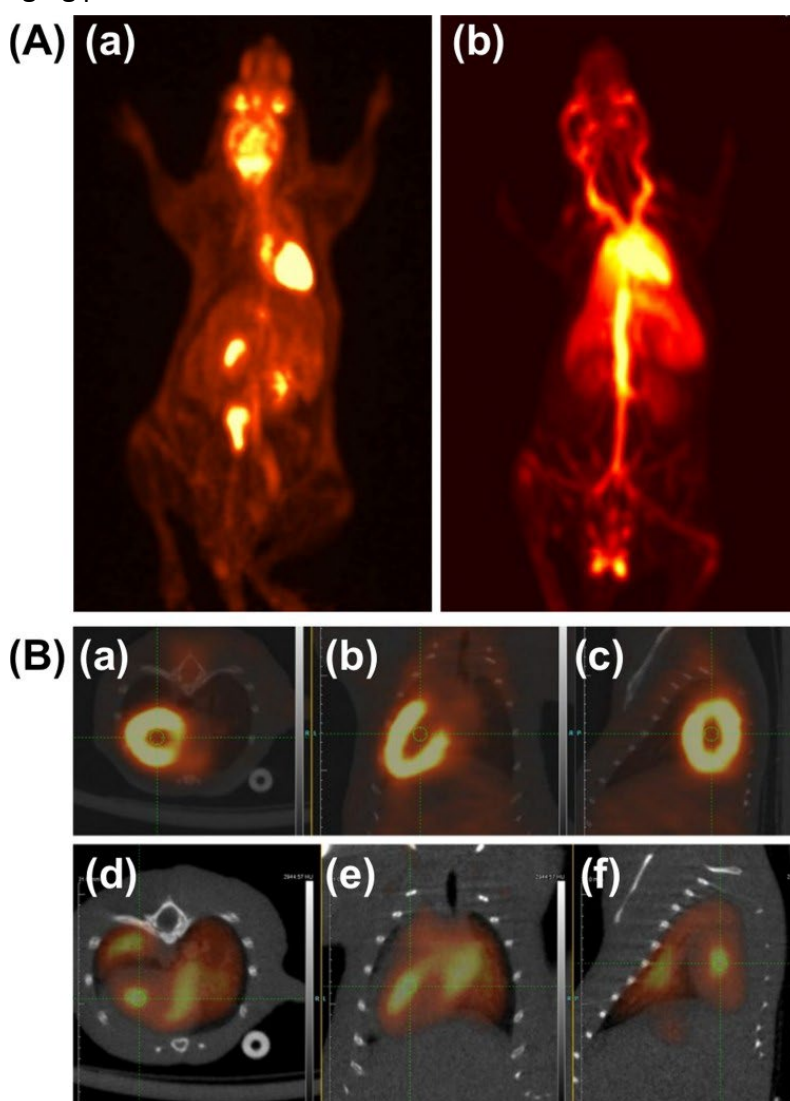


Figure 2. The use of ^{18}F -fluorodeoxyglucose (FDG)-labelled erythrocytes as an *in vivo* imaging probe.

Whole-body positron emission tomography (PET) image of a splenectomised NOD scid gamma (NSG) mouse injected with (a) 1.7 MBq free FDG or (b) 10.4 MBq ^{18}F -FDG-labelled erythrocytes. (B) Axial (left), coronal (middle), and sagittal (right) fused microPET/computed tomography images of the thorax of a splenectomised NSG mouse injected with (a) 2.2 MBq free FDG or (b) 1.7 MBq FDG-labelled human erythrocytes. Reproduced, with permission, from [41]

Once an EIA is generated, its biodistribution can be controlled via active targeting. This can be achieved using sites on the erythrocyte membrane for surface functionalisation. The feasibility of this method was exemplified by erythrocyte membrane-coated Prussian blue nanoparticles. Carboxyl groups present in erythrocyte membranes can be activated using 1-ethyl-3-(3-dimethylaminopropyl)carbodiimide (EDC) combined with *N*-hydroxysuccinimide [40]. Upon the addition of folic acid and amine-containing 1,2-distearoyl-*sn*-glycero-3-phosphoethanolamine PEG (DSPE-PEG-NH₂), surface functionalisation of erythrocyte membrane-coated Prussian blue nanoparticles was reported [40]. Folic acid enabled the coated nanoparticles to successfully target tumour cells in which folic acid receptors were overexpressed [40]. This strategy of targeting ligand incorporation paves the way for the future design of EIAs for molecular imaging.

Engineering and optimisation of EIAs in imaging

To obtain an effective and safe EIA for imaging applications in the living body, multiple factors must be considered. One of these is the compatibility of donor erythrocytes with recipients, particularly with the source of erythrocytes and donor/receiver blood types. Blood-type mismatches can cause transfusion reactions or even death [40]. The time of blood collection is another factor to be noted. The importance of this has been demonstrated in an earlier study [41] in which an imaging agent was loaded into collected erythrocytes for positron emission tomography (PET) of clinical blood pool. Compared with the erythrocytes collected 5 days before loading the agent, those collected within 24 h were more effectively loaded with the imaging agent [41]. Apart from the blood source and collection time, the status of erythrocytes determines the performance of the EIA. This is because when erythrocytes become senescent, catabolic changes occurring inside them cause loss of cell elasticity [42], resulting in a decline in the capacity of ECs to pass through microvessels and an increase in the susceptibility of the generated EIA to be removed by the reticuloendothelial system (RES) [42].

In addition to erythrocytes, the imaging agent to be encapsulated by ECs must be carefully decided during the design stage. Variations in the properties of agents can lead to changes in encapsulation efficiency. This was observed for dextran-based magnetic particles used in magnetic particle imaging (MPI). Compared with perimag nanoparticles, synomag-D nanoparticles exhibited better performance when the same amount of iron was used for EIA generation [43]. Variations in the surface properties of an imaging agent can also lead to changes in the encapsulation efficiency as exemplified in the case of perimag particles. Compared with plain nanoparticles, those surface-functionalised with carboxyl groups were more effective for dose-dependent iron encapsulation by erythrocytes and could fill the erythrocytes in greater amounts [43]. By contrast, perimag particles surface-functionalised with amine groups performed poorly when

encapsulated by erythrocytes than their unmodified counterparts [43]. This demonstrates the importance of proper selection and control of imaging agents when EIAs are being designed.

Careful design of the fabrication process is needed once the erythrocytes and imaging agents are selected. Imaging agents can generally be incorporated into ECs by either attachment to the carrier surface or physical entrapment inside the carrier; however, physical and chemical alterations of the erythrocyte membrane often lead to some degree of membrane damage that can stimulate clotting, apoptosis, and enhanced elimination through the RES. By contrast, loading agents into ECs generally leads to minimal changes in the biodistribution profile unless it leads to changes in the properties (e.g., size, shape, and charge) of the carrier itself [44], and hence, is more preferred. Furthermore, during the optimisation of the fabrication process, the encapsulation efficiency and the sidedness of the erythrocyte membrane on the imaging agent should be considered. This is because the exoplasmic and cytoplasmic sides of the erythrocyte membrane display charge asymmetry, with the exoplasmic side possessing a more negative charge [45]. Therefore, the erythrocyte membrane sidedness may affect the ultimate properties of the EIA. The sidedness of the membrane can be determined by examining the presence and orientation of CD47 on the generated EIA [46]. This can be achieved by incubating conjugated carboxyl-terminated polystyrene microspheres with anti-CD47 antibodies, which can bind specifically to either the exoplasmic or cytoplasmic regions of CD47, with an EIA to observe the presence or absence of binding reactions [46]. Since CD47 interacts with the signal regulatory protein α receptor to inhibit macrophage phagocytosis [46], determining the sidedness of the erythrocyte membrane will help predict the efficiency of the EIA in imaging applications.

Engineering and optimisation at the product level

After optimisation at the design level, the effectiveness of the generated EIA can be further improved at the product level. The physicochemical properties of an imaging agent can change during EIA fabrication as demonstrated using citrate-stabilised gold nanoparticles, whose diameter changed from 70 to 90 nm after being coated with erythrocyte membranes [46]. This increase in diameter was attributed to the membrane width of the erythrocytes. Furthermore, erythrocyte membranes enabled charge screening because the negativity of the surface charge was less than that of citrate-stabilised gold nanoparticles. Therefore, the zeta potential of the nanoparticles changed from approximately -42.2 to -35.1 mV after being coated with erythrocyte membranes [46]. A change in surface charge was noted in Prussian blue nanoparticles whose zeta potential decreased from -5.2 to -15.6 mV after being coated with erythrocyte membranes and conjugated with folic acid [40]. Although the direction of change depends on the original surface properties of the imaging agent,

the impact of erythrocyte membrane concealment on the surface charge of the agent was corroborated.

In addition to changes in the physicochemical properties, camouflaging imaging agents with erythrocyte membranes may alter cellular internalisation. This was reported in a recent study [40] in which an erythrocyte membrane-coated imaging agent was found to enter target cells via caveolae-mediated endocytosis. By contrast, uncoated counterparts triggered actin-mediated membrane ruffling to enter target cells via micropinocytosis[40]. The mechanism underlying this change in cellular uptake is yet to be elucidated. Considering that the process of cellular internalisation affects the implementation of imaging procedures and spatial distribution of imaging signals at cellular and tissue levels, efforts to decipher the underlying mechanism are crucial for more effective optimisation of EIAs in bioimaging.

Status of the use of EIAs in preclinical and clinical settings

The use of EIAs in the preclinical context has been documented for different imaging modalities ranging from fluorescence imaging and MRI to PAI. With the use of ECs, technical problems associated with various imaging techniques are addressed. For instance, the rapid distribution of the paramagnetic gadolinium-based molecular contrast agent between interstitial spaces and plasma in contrast-enhanced MRI increases the signal-to-noise ratio and decreases the size of the imaging window [38]. To address this problem, EIAs were generated using paramagnetic polymeric nano-particles. During the fabrication process, 1,4,7,10-tetraazacyclododecane-1,4,7,10-tetraacetic acid (DOTA) was combined with DSPE with subsequent chelation of Gd^{3+} to the DOTA moiety to obtain a lipid-conjugated gadolinium-based molecular contrast agent [38]. The generated product interacted with PLGA to form a lipid-polymer paramagnetic core [38], which was subsequently concealed within an erythrocyte membrane for use in contrast-enhanced MRI (Figure 3) [38]. The presence of proteins in the outer layer of the membrane coating introduced mass and steric hindrance to the paramagnetic Gd^{3+} ions [38], restricting the rotation of the ions and delaying the molecular tumbling time, leading to contrast enhancement [38]. The longitudinal relaxivity of the core was further facilitated by hydrogen bonds in water molecules trapped by the carbohydrate moieties of the erythrocyte membrane coating [38]. This placed water protons near the paramagnetic Gd^{3+} ions to accelerate water exchange [38]. Compared with commercially available contrast agents which give magnetic resonance (MR) signals mainly in the kidneys [38], the generated EIAs enhanced MR signals in the abdominal aorta, making the delineation of the carotid arteries and superficial blood vessels of the head possible [38]. The MR signal provided by the EIAs in the heart and blood vessels was also stronger than that provided by the commercially available contrast agents [38]. The long-lasting contrast enhancement provided by the EIAs in the heart and blood vessels is mainly attributed to the

ability of the ECs to help the imaging agent stay within the vascular system and exhibit immune evasion. Such ability to prolong the blood circulation time and reduce renal elimination of the contrast agent warrants further exploitation for MRI-mediated vascular imaging in the future.

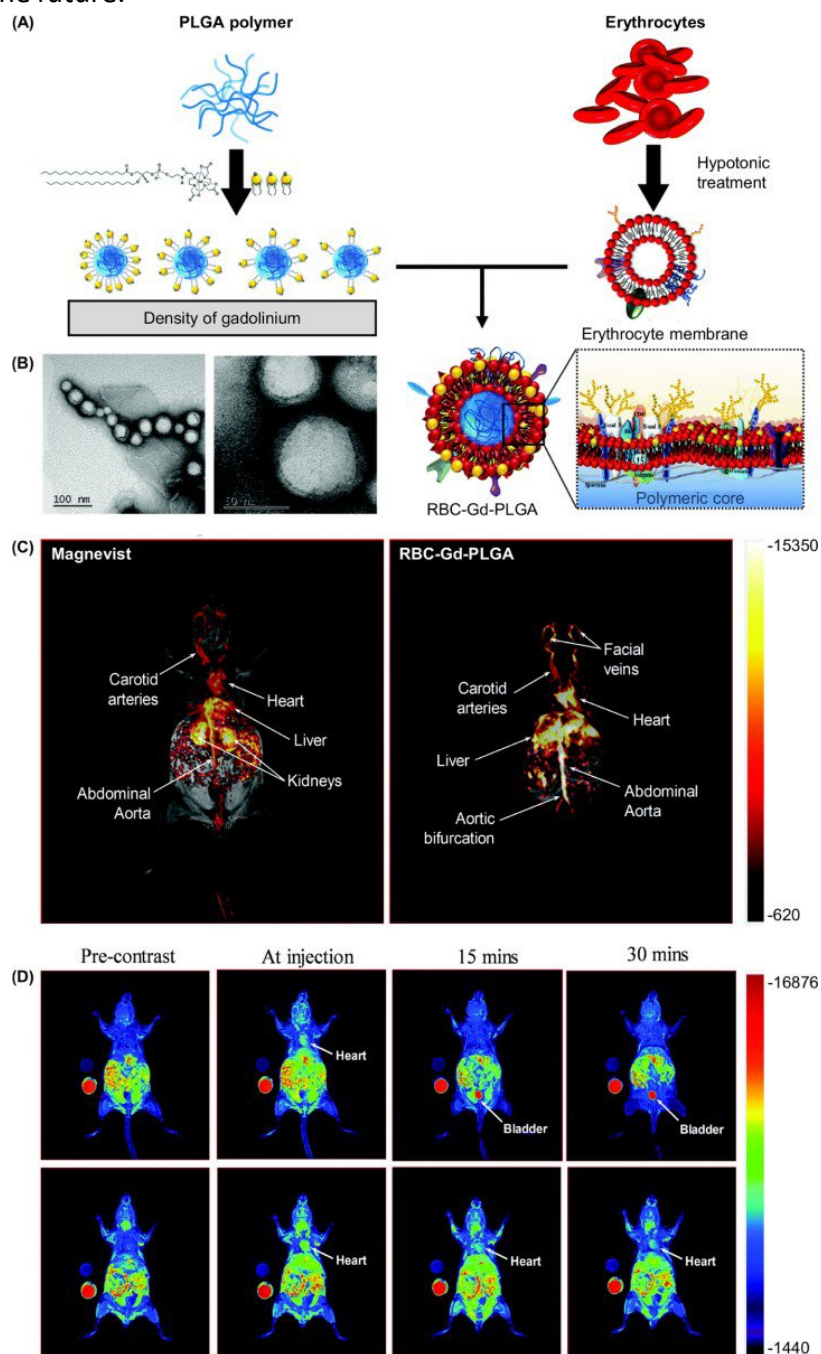


Figure 3. Generation of red blood cell (RBC) membrane-coated paramagnetic nanoparticles consisting of poly(lactic-co-glycolic acid) (PLGA) and a lipid-conjugated gadolinium-based molecular contrast agent for magnetic resonance imaging. (A) A schematic diagram illustrating the process of generating biomimetic paramagnetic nanoconstructs using the erythrocyte membrane, Gd-lipid, and PLGA. (B) Transmission electron microscopic image of the generated nanoconstructs negatively stained with uranyl acetate. Scale bar = 100 nm (left) and 50 nm (right). (C) 3D reconstruction of time-dependent T1-weighted magnetic resonance images obtained using maximum intensity projection with pre- and post-contrast subtraction. (D) Time-dependent 3D reconstruction using maximum intensity projection without pre-contrast subtraction. Reproduced, with permission, from [38]

Apart from enhancing MRI signals, ECs increased the efficiency of other imaging modalities, such as fluorescence imaging and PAI, as corroborated using Prussian blue nanoparticles [47]. These nanoparticles have been widely studied since the turn of the past century because they serve as contrast agents for PAI and have been approved by the FDA for cancer treatment [47]. Furthermore, these nanoparticles showed great potential for theranostic applications [48–50]. To enhance their performance in dealing with cancer, Russian blue nanoparticles were loaded with chemotherapeutic drugs and coated with folic acid-modified erythrocyte membranes [40]. With the use of a cervical tumour xenograft model, the coated nanoparticles were found to remarkably enhance the intensity of PAI signals at the tumour site 36 h post-injection [40]. Compared with their uncoated counterparts, the coated nanoparticles showed a 2–3-fold increase in their half-life in blood upon intravenous administration [40]. Importantly, analysis of the biodistribution profile revealed that the number of nanoparticles found in the heart, liver, spleen, lungs, and kidneys reduced significantly after being concealed with erythrocyte membranes [40]. This indicated that the erythrocyte membrane can help nanoparticles escape from the action of the RES in these organs. The use of ECs for imaging purposes has been tested in preclinical trials for diverse diseases ranging from cancer to myocardial infarction. Additional examples of ECs that have undergone preclinical testing are presented in Table 1 [51–57].

In addition to preclinical applications, ECs demonstrated practical potential in the human body. For instance, autologous erythrocytes loaded with dexamethasone sodium phosphate (DSP) administered to 22 patients with ataxia telangiectasia for 6 months improved their disease status based on the International Cooperative Ataxia Rating Scale (ICARS) [35]. Combining chemotherapy with erythrocyte-encapsulated asparaginase in patients with advanced pancreatic adenocarcinoma showed a higher rate of overall survival (OS) and progression-free survival (PFS) compared with only chemotherapy [37]. This record of human use streamlines the transition of EIAs from laboratory and preclinical contexts to clinical use. Currently, the clinical applications of EIAs largely occur during blood pool imaging, such as autologous human erythrocytes labelled with ^{99m}Tc pertechnetate. These labelled erythrocytes can be imaged using both planar imaging and single-photon emission computed tomography (SPECT) [58]. Upon intravenous administration of labelled erythrocytes along with the use of SPECT/CT fusion imaging techniques, sites of lower gastrointestinal bleeding in patients were successfully detected [58]. This demonstrates the clinical prospects of ECs in diagnosis and provides grounds for the optimisation of EIAs designed for different imaging modalities for clinical trials.

Table 1. Examples of preclinical studies on the use of EIAs for imaging applications

Disease	Details of the EIA	Performance	Refs
Breast cancer	Erythrocyte membrane-coated mesoporous silica nanoparticles containing doxorubicin and chlorin e6	The fluorescence of Ce6 inside the coated nanoparticles enables tumour imaging to be performed in tumour-bearing mice. Meanwhile, laser-activated release of doxorubicin inside the tumours is reported.	[51]
	Erythrocyte-derived vesicles surface-modified with folic acid and fluorescein Cy5	The vesicles show tumour targeting capacity for circulating tumour cell (CTC) capture while enabling fluorescence imaging of the tumour cells.	[52]
	Erythrocyte membrane-coated Fe ₃ O ₄ magnetic nanoparticles	The coated nanoparticles show good magnetic and photothermal properties and are long-lasting in blood circulation. They demonstrate the ability to mediate not only MRI but also photothermal therapy in a preclinical trial.	[53]
	Erythrocytes doped with indocyanine green	The doped erythrocytes enable fluorescence imaging of the tumours and can kill tumour cells in mice via synergistic photochemical and photothermal effects.	[55]
	Erythrocyte membrane-coated iron oxide magnetic clusters	The coated clusters serve as a contrast agent for MRI of the tumours.	[56]
Lung cancer	^{99m} Tc-labelled erythrocytes (surface-modified with cyclic RGD) loaded with gefitinib-loaded albumin nanoparticles	The modified erythrocytes selectively accumulate in the tumour tissues in a lung cancer mouse model and enable real-time imaging of the tumour.	[54]
Myocardial infarction	Erythrocytes doped with indocyanine green	The doped erythrocytes enable the location of atherosclerotic lesions and occlusion caused by myocardial infarction to be detected by using both PAI and fluorescence imaging.	[57]

To date, the imaging function of ECs has been documented in diagnosing and monitoring various physiological conditions that involve abnormalities or alterations in the vasculature, for example, myocardial changes in response to injury and drug action. FDG-labelled erythrocytes combined with PET/CT were used to detect differences in the degree of drug-induced intramyocardial vasodilation between diabetic rats and normal controls [59], and to locate the area of myocardial injury in a surgical myocardial infarction rat model [59]. Another example is cancer that is characterised by leaky vasculature. Encapsulating gefitinib-loaded albumin nanoparticles using ⁹⁹Tc-labelled cyclic arginylglycylaspartic acid (RGD)-modified erythrocyte membranes enabled the nanoparticles to effectively escape phagocytosis upon injection into the body and selectively accumulate in the tumour tissues to enable real-time tumour imaging [54]. Similar success in EC-mediated tumour imaging was reported by Burns *et al.* [60] who generated light-activated nanoparticles using erythrocytes. They noted that the nanoparticles accumulated in larger amounts in tumours than in organs and revealed the potential of the nanoparticles to serve as imaging probes for near-IR fluorescence imaging of tumours during cytoreductive surgery. Recently, under high-resolution photoacoustic microscopy, ECs were used to successfully image blood vessels in the ears of BALB/c mice. The details and branches of venules and arterioles were identified, and single erythrocytes inside the vessels were also imaged [61]. In addition to the aforementioned examples, EC-mediated imaging has been used to examine retinal microcirculation [62,63], intracranial haemorrhage [64], and ischaemic stroke [65]. All these examples demonstrate the high practical potential of ECs in imaging applications.

Concluding remarks and future perspectives

Erythrocytes are physiological entities that have been exploited in both preclinical and clinical trials as carriers of exogenous agents. Numerous ECs have been documented in the literature [66,67], and several of them show promising potential for use in imaging because of their favourable properties, ranging from possible plastic deformability to high biocompatibility. With advances in the development and engineering of ECs, the design of EIAs is expected to shift from monofunctional to multifunctional. This trend has already started as evidenced by the emergence of different ECs that integrate imaging with therapy [53,55]. Even for EIAs designed solely for imaging purposes, efforts have been made to integrate multiple imaging modalities into one design. This was partially exemplified by near-IR erythrocyte-derived transducers, which were generated by loading erythrocyte ghosts with indocyanine green for PAI [57]. Transducers were reported to accumulate in inflamed tissues (via integrin- and complement-based adherence to damaged endothelium and monocytes) [57] and enabled the detection of myocardial infarction by both PAI and fluorescence imaging [57]. Such high versatility in the function of an imaging

agent is expected to become a major focus of imaging research over the next decade. With the well-supported application potential of ECs, as shown in preclinical and clinical trials, it is expected that an increasing number of EIAs will enter clinical trials soon. An increase in investment in EIA-related research and development activities in the industrial sector is also anticipated. This increase started over the past several decades with multiple EIAs being patented for industrial and commercial purposes (Table 2) [68–82]. Although discussions in this article focus on ECs, other blood components, including granulocytes and platelets, also have the potential to be used for designing imaging probes and have been patented for their commercial potential. Technical questions still need to be addressed before EIAs can be applied extensively to routine clinical practice (see Outstanding questions), but a solid foundation for the clinical translation of these agents has been established by the track record of the clinical use of erythrocytes and their derived products. Along with rapid advances in imaging technologies [83–89] and the continuous increase in the sophistication of techniques for fabricating, engineering, and optimising properties of ECs, the emergence of more effective EIAs with promising application potentials is close.

Table 2. Examples of patents on imaging probes whose production involves the use of erythrocytes or other blood components

Patent number	Patent title	Description of the invention	Anticipated expiration date	Refs
EP3372250B1	Methods for production and use of substance-loaded erythrocytes for observation and treatment of microvascular hemodynamics	This patent reports the preparation of erythrocytes pre-loaded with imaging agents (which enable the observation of blood flow under physiological conditions) for detection of circulation abnormalities.	1 May 2029	[68–71]
EP2285421B1				
ES2671710T3				
US10041042B2				
US5328840A	Method for preparing targeted carrier erythrocytes	This patent reports the preparation of erythrocytes conjugated with targeting ligands for possible imaging applications. The erythrocytes can react with activated platelets in a thrombus, and be loaded with different imaging agents to enable the thrombus to be visualised. The imaging agent that can be incorporated into the carrier erythrocytes includes heavy metal contrast agents for X-ray imaging, MRI agents, and radioactive nuclides for radioimaging.	12 July 2011	[72]
US4755375A	Method and kit for the selective labelling of red blood cells in whole blood with TC-99M	This patent reports a method of preparation of ^{99m} Tc-labelled erythrocytes for applications such as blood pool imaging and spleen imaging.	5 July 2005	[73]
US4313928A	Composition for labelling of red blood cells with radioactive technetium	This patent provides a composition for attaining efficient intracorporeal ^{99m} Tc labelling of erythrocytes.	19 November 1999	[74]
US5045304A	Contrast agent having an imaging agent coupled to viable granulocytes for use in MRI of abscess and a method of preparing and using same	This patent reports the use of granulocytes separated from whole blood for encapsulation of a contrast agent for MRI	3 September 2008	[75]
US5332578A	Platelet membrane microparticles	This patent reports a method to generate heat-treated, viral-inactivated platelet membrane microparticles, which can subsequently be labelled with imaging moieties so as to serve as an imaging agent to trace the location of a clot.	26 July 2011	[76]
US8512697B2	Delivery of micro- and nanoparticles with blood platelets	This patent reports a method to generate palettes loaded with imaging agents for imaging sites of vascular injury.	12 August 2030	[77]
AU2010234607B2	Spray-dried blood products and methods of making same	This patent reports a method to produce spray-dried blood products for delivery of substances ranging from drugs to imaging agents.	6 April 2030	[78–81]
CA2757961C				
ES2684130T3				
EP2416790B1				
US9867782B2			15 February 2034	[82]

Declaration of interests

No interests are declared.

References

1. Obireddy, S.R. and Lai, W.F. (2021) Multi-component hydrogel beads incorporated with reduced graphene oxide for pH responsive and controlled co-delivery of multiple agents. *Pharmaceutics* 13, 313
2. Lai, W.F. et al. (2021) Alginate-based complex fibers with the Janus morphology for controlled release of co-delivered drugs. *Asian J. Pharm. Sci.* 16, 77–85
3. Lai, W.F. (2022) Non-aromatic clusteroluminogenic polymers: structural design and applications in bioactive agent delivery. *Mater. Today Chem.* 23, 100712
4. Zheng, S. et al. (2018) Noninvasive photoacoustic and fluorescent tracking of optical dye labeled T cellular activities of diseased sites at new depth. *J. Biophotonics* 11, e201800073
5. Chen, R.H. et al. (2021) Photoacoustic molecular imaging escorted adipose photodynamic-browning synergy for fighting obesity with virus-like complexes. *Nat. Nanotechnol.* 16, 455–465
6. Wang, C. et al. (2021) Construction and evaluation of red blood cells-based drug delivery system for chemo-photothermal therapy. *Colloids Surf. B Biointerfaces* 204, 111789
7. Malhotra, S. et al. (2019) Red blood cells-derived vesicles for delivery of lipophilic drug camptothecin. *ACS Appl. Mater. Inter.* 11, 22141–22151
8. Han, X. et al. (2019) Red blood cell-derived nanoerythroosome for antigen delivery with enhanced cancer immunotherapy. *Sci. Adv.* 5, eaaw6870
9. Della Pelle, G. and Kostevsek, N. (2021) Nucleic acid delivery with red-blood-cell-based carriers. *Int. J. Mol. Sci.* 22, 5264
10. Borgheti-Cardoso, L.N. et al. (2020) Extracellular vesicles derived from Plasmodium-infected and non-infected red blood cells as targeted drug delivery vehicles. *Int. J. Pharmaceut.* 587, 119627
11. Bidkar, A.P. et al. (2020) Transferrin-conjugated red blood cell membrane-coated poly(lactic-co-glycolic acid) nanoparticles for the delivery of doxorubicin and methylene blue. *ACS Appl. Nano Mater.* 3, 3807–3819
12. Yuan, J. et al. (2021) Cargo-laden erythrocyte ghosts target liver mediated by macrophages. *Transfus. Apher. Sci.* 60, 102930
13. Xia, Q. et al. (2019) Red blood cell membrane-camouflaged nanoparticles: a novel drug delivery system for antitumor application. *Acta Pharm. Sin. B* 9, 675–689
14. Liu, X.L. et al. (2020) Haemoglobin-loaded metal organic framework-based nanoparticles camouflaged with a red blood cell membrane as potential oxygen

delivery systems. *Biomater. Sci.* 8, 5859–5873

15. Soliman, M.M. et al. (2021) Polyethylene oxide-polyacrylic acid-folic acid (PEO-PAAC) nanogel as a Tc-99m targeting receptor for cancer diagnostic imaging. *J. Labelled Compd. Rad.* 64, 534–547

16. Mandal, T.K. et al. (2021) pH-Responsive biocompatible fluorescent core-shell nanogel for intracellular imaging and control drug release. *Part. Part. Syst. Charact.* 38, 2100110

17. Kimura, A. et al. (2021) Ultra-small size gelatin nanogel as a blood brain barrier impermeable contrast agent for magnetic resonance imaging. *Acta Biomater.* 125, 290–299

18. Lai, W.F. and Wong, W.T. (2018) Design of polymeric gene carriers for effective intracellular delivery. *Trends Biotechnol.* 36, 713–728

19. Lai, W.F. and Shum, H.C. (2016) A stimuli-responsive nanoparticulate system using poly(ethylenimine)-graft-polysorbate for controlled protein release. *Nanoscale* 8, 517–528

20. Ma, H. et al. (2022) Mn-dox metal-organic nanoparticles for cancer therapy and magnetic resonance imaging. *Dyes Pigments* 199, 110080

21. Lai, W.F. et al. (2020) Development of copper nanoclusters for in vitro and in vivo theranostic applications. *Adv. Mater.* 32, e1906872

22. Magar, K.T. et al. (2022) Liposome-based delivery of biological drugs. *Chin. Chem. Lett.* 33, 587–596

23. Turchin, I. et al. (2022) Combined fluorescence and optoacoustic imaging for monitoring treatments against CT26 tumors with photoactivatable liposomes. *Cancers* 14, 197

24. Medina, T.P. et al. (2022) Utilizing sphingomyelinase sensitizing liposomes in imaging intestinal inflammation in dextran sulfate sodium-induced murine colitis. *Biomedicines* 10, 413

25. Lai, W.F. et al. (2020) Molecular design of layer-by-layer functionalized liposomes for oral drug delivery. *ACS Appl. Mater. Inter.* 12, 43341–43351

26. Khoshnejad, M. et al. (2018) Ferritin-based drug delivery systems: Hybrid nanocarriers for vascular immunotargeting. *J. Control. Release* 282, 13–24

27. Dhanasooraj, D. et al. (2013) Vaccine delivery system for tuberculosis based on nano-sized hepatitis B virus core protein particles. *Int. J. Nanomedicine* 8, 835–843

28. Zhu, R.X. et al. (2021) In vivo nano-biosensing element of red blood cell-mediated delivery. *Biosens. Bioelectron.* 175, 112845

29. Wan, X. et al. (2019) Red blood cell-derived nanovesicles for safe and efficient macrophage-targeted drug delivery in vivo. *Biomater. Sci.* 7, 187–195

30. Glassman, P.M. et al. (2020) Vascular drug delivery using carrier red blood cells:

focus on RBC surface loading and pharmacokinetics. *Pharmaceutics* 12, 440

31. Ferguson, L. et al. (2021) Targeted drug delivery to the pulmonary endothelium using liposomal nanocarriers and red blood cell super carriers. *Am. J. Resp. Crit. Care* 203, 1277752
32. Bian, H. et al. (2022) Erythrocyte ghost based fusogenic glycoprotein vesicular stomatitis virus glycoprotein complexes as an efficient deoxyribonucleic acid delivery system. *J. Biomater. Tiss. Eng.* 12, 1080–1086
33. Hunault-Berger, M. et al. (2015) A phase 2 study of Lasparaginase encapsulated in erythrocytes in elderly patients with Philadelphia chromosome negative acute lymphoblastic leukemia: the GRASPALL/GRAALL-SA2-2008 study. *Am. J. Hematol.* 90, 811–818
34. Bax, B.E. et al. (2000) In vitro and in vivo studies with human carrier erythrocytes loaded with polyethylene glycol-conjugated and native adenosine deaminase. *Brit. J. Haematol.* 109, 549–554
35. Chessa, L. et al. (2014) Intra-erythrocyte infusion of dexamethasone reduces neurological symptoms in ataxia teleangiectasia patients: results of a phase 2 trial. *Orphanet. J. Rare Dis.* 9, 5
36. Bax, B.E. et al. (2019) Erythrocyte encapsulated thymidine phosphorylase for the treatment of patients with mitochondrial neurogastrointestinal encephalomyopathy: study protocol for a multi-centre, multiple dose, open label trial. *J. Clin. Med.* 8, 1096
37. Hammel, P. et al. (2020) Erythrocyte-encapsulated asparaginase (eryaspase) combined with chemotherapy in second-line treatment of advanced pancreatic cancer: an open-label, randomized Phase IIb trial. *Eur. J. Cancer* 124, 91–101
38. Nguyen, T.D.T. et al. (2020) Erythrocyte membrane concealed paramagnetic polymeric nanoparticle for contrast-enhanced magnetic resonance imaging. *Nanoscale* 12, 4137–4149
39. Yang, Q. et al. (2019) Erythrocyte membrane-camouflaged IR780 and DTX co-loading polymeric nanoparticles for imagingguided cancer photo-chemo combination therapy. *Mol. Pharm.* 16, 3208–3220
40. Xiao, F. et al. (2019) An erythrocyte membrane coated mimetic nano-platform for chemo-phototherapy and multimodal imaging. *RSC Adv.* 9, 27911–27926
41. Choi, J.W. et al. (2019) In vivo positron emission tomographic blood pool imaging in an immunodeficient mouse model using ¹⁸F-fluorodeoxyglucose labeled human erythrocytes. *PLoS One* 14, e0211012
42. Li, Y.C. et al. (2021) Clinical progress and advanced research of red blood cells based drug delivery system. *Biomaterials* 279, 121202
43. Antonelli, A. et al. (2020) Development of long circulating magnetic particle imaging tracers: use of novel magnetic nanoparticles and entrapment into human

erythrocytes. *Nanomedicine* 15, 739–753

44. Sylvestre, M. et al. (2020) Progress on modulating tumor-associated macrophages with biomaterials. *Adv. Mater.* 32, e1902007

45. Spiess, M. (1995) Heads or tails — what determines the orientation of proteins in the membrane. *FEBS Lett.* 369, 76–79

46. Gao, W.W. et al. (2013) Surface functionalization of gold nanoparticles with red blood cell membranes. *Adv. Mater.* 25, 3549–3553

47. Liang, X.L. et al. (2013) Prussian blue nanoparticles operate as a contrast agent for enhanced photoacoustic imaging. *Chem. Commun.* 49, 11029–11031

48. Mamontova, E. et al. (2020) Fashioning prussian blue nanoparticles by adsorption of luminophores: synthesis, properties, and in vitro imaging. *Inorg. Chem.* 59, 4567–4575

49. Cano-Mejia, J. et al. (2020) CpG-coated prussian blue nanoparticles-based photothermal therapy combined with anti-CTLA-4 immune checkpoint blockade triggers a robust abscopal effect against neuroblastoma. *Transl. Oncol.* 13, 100823

50. Busquets, M.A. and Estelrich, J. (2020) Prussian blue nanoparticles: synthesis, surface modification, and biomedical applications. *Drug Discov. Today* 25, 1431–1443

51. Su, J. et al. (2017) Enhanced blood suspensibility and laser-activated tumor-specific drug release of theranostic mesoporous silica nanoparticles by functionalizing with erythrocyte membranes. *Theranostics* 7, 523–537

52. Chen, M. et al. (2019) Erythrocyte-derived vesicles for circulating tumor cell capture and specific tumor imaging. *Nanoscale* 11, 12388–12396

53. Rao, L. et al. (2017) Microfluidic electroporation-facilitated synthesis of erythrocyte membrane-coated magnetic nanoparticles for enhanced imaging-guided cancer therapy. *ACS Nano* 11, 3496–3505

54. Wen, Q. et al. (2021) Erythrocyte-membrane-camouflaged gefitinib/albumin nanoparticles for tumor imaging and targeted therapy against lung cancer. *Int. J. Biol. Macromol.* 193, 228–237

55. Burns, J.M. et al. (2018) Erythrocyte-derived theranostic nanoplateforms for near infrared fluorescence imaging and photodestruction of tumors. *ACS Appl. Mater. Interfaces* 10, 27621–27630

56. Ren, X. et al. (2016) Red blood cell membrane camouflaged magnetic nanoclusters for imaging-guided photothermal therapy. *Biomaterials* 92, 13–24

57. Liu, Y.G. et al. (2020) Non-invasive photoacoustic imaging of in vivo mice with erythrocyte derived optical nanoparticles to detect CAD/MI. *Sci. Rep.* 10, 5983

58. Wang, Z.G. et al. (2015) Technological value of SPECT/CT fusion imaging for the diagnosis of lower gastrointestinal bleeding. *Genet. Mol. Res.* 14, 14947–14955

59. Wang, S.W. et al. (2022) In vivo imaging of rat vascularity with FDG-labeled erythrocytes. *Pharmaceuticals* 15, 292
60. Burns, J.M. et al. (2021) Near infrared fluorescence imaging of intraperitoneal ovarian tumors in mice using erythrocyte-derived optical nanoparticles and spatially-modulated illumination. *Cancers* 13, 2544
61. He, G. et al. (2015) In vivo imaging of a single erythrocyte with high-resolution photoacoustic microscopy. *Front. Optoelectron.* 8, 122–127
62. Gu, B.Y. et al. (2018) Noninvasive in vivo characterization of erythrocyte motion in human retinal capillaries using high-speed adaptive optics near-confocal imaging. *Biomed. Opt. Express* 9, 3653–3677
63. Pottenburgh, J. et al. (2020) Use of FITC and CFSE labeled erythrocytes for in vivo retinal imaging in non-human primates. *Invest. Ophthalmol. Vis. Sci.* 61, 897
64. Wang, Y. et al. (2017) ¹⁸F-positron-emitting/fluorescent labeled erythrocytes allow imaging of internal hemorrhage in a murine intracranial hemorrhage model. *J. Cerebr. Blood F Met.* 37, 776–786
65. Vankayala, R. et al. (2018) Erythrocyte-derived nanoparticles as a theranostic agent for near-infrared fluorescence imaging and thrombolysis of blood clots. *Macromol. Biosci.* 18, e1700379
66. Zhang, X.B. et al. (2021) Erythrocyte membrane-camouflaged carrier-free nanoassembly of FRET photosensitizer pairs with high therapeutic efficiency and high security for programmed cancer synergistic phototherapy. *Bioact. Mater.* 6, 2291–2302
67. Yao, Q. et al. (2021) Aging erythrocyte membranes as biomimetic nanometer carriers of liver-targeting chromium poisoning treatment. *Drug Deliv.* 28, 1455–1465
68. Flower, R.W. Methods for production and use of substanceloaded erythrocytes for observation and treatment of microvascular hemodynamics, ES2671710T3
69. Flower, R.W. Methods for production and use of substanceloaded erythrocytes (S-IEs) for observation and treatment of microvascular hemodynamics, US10041042B2
70. Flower, R.W. Methods for production and use of substanceloaded erythrocytes for observation and treatment of microvascular hemodynamics, EP3372250B1
71. Flower, R.W. Methods for production and use of substanceloaded erythrocytes for observation and treatment of microvascular hemodynamics, EP2285421B1
72. Coller, B.S. Method for preparing targeted carrier erythrocytes, US5328840A
73. Srivastava, S.C. et al. Method and kit for the selective labeling of red blood cells in whole blood with TC-99M, US4755375A
74. Kato, M. and Hazue, M. Composition for labeling of red blood cells with radioactive technetium, US4313928A

75. Schneider, D.R. and Bis, K.G. Contrast agent having an imaging agent coupled to viable granulocytes for use in magnetic resonance imaging of abscess and a method of preparing and using same, US5045304A
76. Chao, F. Platelet membrane microparticles, US5332578A
77. Fischer, T.H. et al. Delivery of micro- and nanoparticles with blood platelets, US8512697B2
78. Dacorta, J.A. et al. Spray-dried blood products and methods of making same, ES2684130T3
79. Dacorta, J.A. et al. Spray-dried blood products and methods of making same, CA2757961C
80. Dacorta, J.A. et al. Spray-dried blood products and methods of making same, AU2010234607B2
81. Dacorta, J.A. et al. Spray-dried blood products and methods of making same, EP2416790B1
82. Dacorta, J.A. et al. Spray-dried blood products and methods of making same, US9867782B2
83. Xu, Q. et al. (2020) Multi-task joint learning model for segmenting and classifying tongue images using a deep neural network. *IEEE J. Biomed. Health Inform.* 24, 2481–2489
84. Zhang, Z. et al. (2022) Endoscope image mosaic based on pyramid ORB. *Biomed. Signal. Process. Control* 71, 103261
85. Liu, S. et al. (2022) 2D/3D multimode medical image registration based on normalized cross-correlation. *Appl. Sci.* 12, 2828
86. Liu, Y. et al. (2022) Improved feature point pair purification algorithm based on sift during endoscope image stitching. *Front. Neurobot.* 16, 840594
87. Zhang, T. et al. (2022) Transcranial focused ultrasound stimulation of periaqueductal gray for analgesia. *IEEE Trans. Biomed. Eng.* Published online March 24, 2022. <https://doi.org/10.1109/TBME.2022.3162073>
88. Zhang, T. et al. (2022) Piezoelectric ultrasound energy-harvesting device for deep brain stimulation and analgesia applications. *Sci. Adv.* 8, eabk0159
89. Tang, W. et al. (2018) Tumor origin detection with tissue-specific miRNA and DNA methylation markers. *Bioinformatics* 34, 398–406
90. Pierige, F. et al. (2008) Cell-based drug delivery. *Adv. Drug Deliv. Rev.* 60, 286–295
91. Gutierrez Millan, C. et al. (2004) Factors associated with the performance of carrier erythrocytes obtained by hypotonic dialysis. *Blood Cells Mol. Dis.* 33, 132–140
92. Hamidi, M. et al. (2007) Preparation and in vitro evaluation of carrier erythrocytes

- for RES-targeted delivery of interferon- α 2b. *Int. J. Pharm.* 341, 125–133
93. Seth, M. et al. (2010) Dilution technique to determine the hydrodynamic volume fraction of a vesicle suspension. *Langmuir* 26, 15169–15176
94. Magnani, M. et al. (2002) Erythrocyte-mediated delivery of drugs, peptides and modified oligonucleotides. *Gene Ther.* 9, 749–751
95. Lynch, A.L. et al. (2011) pH-responsive polymers for trehalose loading and desiccation protection of human red blood cells. *Biomaterials* 32, 4443–4449
96. Liu, X. et al. (2021) Robust three-dimensional nanotube-in-micropillar array electrodes to facilitate size independent electroporation in blood cell therapy. *Lab Chip* 21, 4196–4207
97. Nicolau, C. and Gersonde, K. (1979) Incorporation of inositol hexaphosphate into intact red blood cells. I. Fusion of effector-containing lipid vesicles with erythrocytes. *Naturwissenschaften* 66, 563–566
98. Kwon, Y.M. et al. (2009) L-Asparaginase encapsulated intact erythrocytes for treatment of acute lymphoblastic leukemia (ALL). *J. Control. Release* 139, 182–189